^{13}C NMR Characterization of an Exchange Reaction between CO and CO_2 Catalyzed by Carbon Monoxide Dehydrogenase[†]

Javier Seravalli[‡,§] and Stephen W. Ragsdale*[,‡,||]

Department of Biochemistry, University of Nebraska, Lincoln, Nebraska 68588, and Department of Biological Chemistry, University of Michigan, Ann Arbor, Michigan 48109-0606

Received March 17, 2008; Revised Manuscript Received April 21, 2008

ABSTRACT: Carbon monoxide dehydrogenase (CODH) catalyzes the reversible oxidation of CO to CO_2 at a nickel−iron−sulfur cluster (the C-cluster). CO oxidation follows a ping-pong mechanism involving two-electron reduction of the C-cluster followed by electron transfer through an internal electron transfer chain to external electron acceptors. We describe ^{13}C NMR studies demonstrating a CODH-catalyzed steady-state exchange reaction between CO and CO_2 in the absence of external electron acceptors. This reaction is characterized by a CODH-dependent broadening of the ^{13}CO NMR resonance; however, the chemical shift of the ^{13}CO resonance is unchanged, indicating that the broadening is in the slow exchange limit of the NMR experiment. The ^{13}CO line broadening occurs with a rate constant (1080 s^{-1} at 20 °C) that is approximately equal to that of CO oxidation. It is concluded that the observed exchange reaction is between ^{13}CO and CODH-bound $^{13}CO_2$ because ^{13}CO line broadening is pH-independent (unlike steady-state CO oxidation), because it requires a functional C-cluster (but not a functional B-cluster) and because the $^{13}CO_2$ line width does not broaden. Furthermore, a steady-state isotopic exchange reaction between ^{12}CO and $^{13}CO_2$ in solution was shown to occur at the same rate as that of CO_2 reduction, which is approximately 750-fold slower than the rate of ^{13}CO exchange broadening. The interaction between CODH and the inhibitor cyanide (CN^-) was also probed by ^{13}C NMR. A functional C-cluster is not required for $^{13}CN^-$ broadening (unlike for ^{13}CO), and its exchange rate constant is 30-fold faster than that for ^{13}CO. The combined results indicate that the ^{13}CO exchange includes migration of CO to the C-cluster, and CO oxidation to CO_2, but not release of CO_2 or protons into the solvent. They also provide strong evidence of a CO_2 binding site and of an internal proton transfer network in CODH. $^{13}CN^-$ exchange appears to monitor only movement of CN^- between solution and its binding to and release from CODH.

Carbon monoxide dehydrogenase (CODH) catalyzes the reversible oxidation of CO to CO_2 according to eq 1.

$$CO + H_2O \leftrightarrow CO_2 + 2H^+ + 2e- \quad (1)$$

In carboxydotrophic microbes, like the hydrogenogenic thermophile *Carboxydothermus hydrogenoformans*, the oxidation of CO is utilized as the sole source of carbon and energy during chemolithoautotrophic growth (*2–4*). There are three classes of CODH: a copper molybdopterin enzyme (*5*) and two classes of Ni enzymes, which have been a primary focus because of their high catalytic activity and importance in anaerobic CO and CO_2 fixation (*6*). A monofunctional Ni-CODH has been characterized from *Rhodospirillum rubrum* (*7, 8*) and *C. hydrogenoformans* (*9*), which reversibly oxidizes CO to CO_2. Association of the monofunctional CODH with another Ni enzyme called acetyl-CoA synthase (ACS) forms a machine called CODH/ACS that converts CO_2, a methyl group (donated by a methylated corrinoid iron−sulfur protein), and CoA to acetyl-CoA, which is the key step in anaerobic CO and CO_2 fixation by the Wood−Ljungdahl pathway (*6, 10, 11*). The overall structures of the CODH component of CODH/ACS and the monofunctional CODH are virtually identical (*8, 9, 12–14*) in which CODH forms an essential homodimeric unit, with each dimer containing two C-clusters, two B-clusters, and one D-cluster. The C-cluster is the catalytic site for CO oxidation and is buried 18 Å below the surface. This cluster can be described as a [3Fe-4S] cluster bridged to a binuclear NiFe cluster; the B-cluster is a typical $[4Fe\text{-}4S]^{2+/1+}$ cluster, and the D-cluster is a $[4Fe\text{-}4S]^{2+/1+}$ cluster that bridges the two subunits, similar to the $[4Fe\text{-}4S]^{2+/1+}$ cluster in the iron protein of dinitrogenase (*15, 16*). CODH follows a ping-pong mechanism, indicating that release of CO_2 precedes the binding of electron acceptors (*17–19*). As we conceive the mechanism, CO binds to and reduces the C-cluster by two electrons, forming CO_2 and two protons (*8, 11, 20*). Then, the two electrons are transferred to the B- and D-clusters, which form an internal redox chain between the C-cluster and external electron acceptors, such as ferredoxin (*14, 18, 19, 21*). The enzymatic reaction is reversible and

[†] This work was partly supported by NIH Grant GM 39451 to S.W.R.

* To whom correspondence should be addressed: Department of Biological Chemistry, University of Michigan, University of Michigan Medical School, 5301 MSRB III, 1150 W. Medical Center Dr., Ann Arbor, MI 48109-0606. Phone: (734) 615-4621. Fax: (734) 763-4581. E-mail: sragsdal@umich.edu.

[‡] University of Nebraska.

[§] Current address: Biological Process Development Facility, Department of Chemical Engineering, University of Nebraska, Lincoln, NE 68588.

[||] University of Michigan.

10.1021/bi8004522 CCC: $40.75
Published on Web 06/10/2008

occurs at the thermodynamic potential, unlike most chemical catalysts, which require a significant overpotential (*22*).

To improve our understanding of the mechanism of oxidation of CO to CO_2, it is important to study the intermediate chemical steps in the reaction. The thermophilic *C. hydrogenoformans* CODH is highly active and, among the monofunctional CODHs, has been structurally characterized in the most detail (*9, 14*). Transient kinetic experiments, like stopped flow UV−visible or fluorescence spectroscopy or rapid freeze quench EPR, are often used to identify the intermediate steps in an enzymatic reaction; however, these experiments rely on the particular step under study occurring more slowly than the mixing time for the instrument, i.e., the half-time for the reaction under study must be longer than the dead time for mixing the enzyme and substrate. CO oxidation by CODH-II[1] from *C. hydrogenoformans* has a rate constant of ~40000 s^{-1} under optimal conditions at 70 °C (*2*) (~500 s^{-1} at 10 °C); therefore, even at 10 °C, the half-time for the overall CO oxidation reaction (~1.4 ms) is too short for most transient kinetic methods (2−10 ms). However, it is apparent that, since CO oxidation is a ping-pong reaction, one should be able to observe the interconversion between CO and CO_2 in the absence of electron acceptors by following an exchange reaction between CO and CO_2. Furthermore, this reaction occurs within the time scale for NMR (10^{-4}−10^4 s). Thus, we used FT-NMR spectroscopy to study the CO−CO_2 exchange reaction with the CODH-II from *C. hydrogenoformans*. Potentially, this reaction could provide more direct information about the chemical steps involved in CO oxidation than measurements that monitor redox reactions, such as reduction of the internal (B-clusters) or external redox acceptors.

There is a precedent for the use of ^{13}C NMR for studying exchange reactions. The equilibrium exchange between CO_2 and HCO_3^-, catalyzed by carbonic anhydrase, has been studied by ^{13}C NMR methods (*23–26*). This exchange is shown to be pH-independent, in contrast to the sharp pH dependence observed for k_{cat} in the steady-state hydration and dehydration reactions (*27*). This difference is attributed to the involvement of an internal proton transfer network with no release of protons to the solution during the exchange reaction, while the steady-state reaction requires the release of a proton to the solvent (*28*). In nonenzymatic reactions, an isotopic exchange between CO and CO_2 in the gas phase has been studied by mass spectrometry (*29*) and by ^{14}C exchange (*30*); however, no studies of the exchange between CO and CO_2 have yet been reported for an enzyme, to the best of our knowledge.

We demonstrate by ^{13}C NMR that free CO undergoes a slow isotopic exchange with free CO_2 or free HCO_3^- in solution and a 500-fold faster ^{13}CO line broadening that is assigned to an exchange reaction between CO and enzyme-bound CO_2. The rapid exchange broadening is dependent on the CODH-II concentration but is independent of the buffer concentration and the pH, and it shows a rather modest (0.87) solvent isotope effect, suggesting that the two protons produced during CO oxidation remain bound at the active site as part of an internal proton transfer network. In contrast, the steady-state CO oxidation reaction exhibits a sharp pH dependence ($pK_a \sim 6.70$). On the basis of mutagenesis and metal depletion experiments, it is shown that the ^{13}CO exchange broadening requires a functional C-cluster, but not a functional B-cluster, indicating that the two electrons produced during CO oxidation remain associated with the C-cluster during the exchange. Electrons are then transferred to the internal electron transfer chain, perhaps associated and/or coordinated with proton transfer, in a subsequent reaction. These results also imply that reduction of bound CO_2 at the C-cluster of CODH-II must occur much faster than the reduction of CO_2 in solution.

MATERIALS AND METHODS

Materials. CO (99.99%) and N_2 (99.998%) were purchased from Linweld (Lincoln, NE). ^{13}C-enriched $NaHCO_3$, CO, and KCN as well as D_2O (all >99.9% isotopically enriched) were purchased from Cambridge Isotopes (Andover, MA). All other chemicals were obtained from Sigma-Aldrich (St. Louis, MO) and were of the highest available purity. Primers were synthesized and HPLC-purified by IDT, Inc. (Coralville, IA). Restriction enzymes, DNA ligase, alkaline phosphatase, and competent cells were purchased from Invitrogen (Carlsbad, CA).

Purification of Native and Recombinant Forms of CODH-II. C. hydrogenoformans (strain DSMZ 6008) was grown with CO as the carbon source at 66 °C as described previously (*2*). CODH-II was purified to >95% homogeneity under strictly anaerobic conditions as previously described (*31*) in a Vacuum Atmospheres (Hawthorne, CA) anaerobic chamber maintained at 18 °C at an oxygen tension of <1 ppm, monitored continuously with a model 317 trace oxygen analyzer (Teledyne Analytical Instruments, City of Industry, CA). The specific activity of purified CODH-II was between 1700 and 2000 units/mg at 30 °C with 1 atm of CO, 20 mM methyl viologen, 50 mM HEPES (pH 8.0), and 2 mM dithiothreitol. Protein concentrations were determined by the Rose Bengal method (*32*) with chicken egg lysozyme as the standard.

Recombinant CODH-II was expressed in *Escherichia coli* BL21(DE3). The *cooSII* gene was amplified from genomic DNA isolated from *C. hydrogenoformans* (*4*) using the *Pfu Turbo* DNA polymerase kit from Stratagene (La Jolla, CA) and the primers 2350N (ACATGCATGCTAGCTAAG-CAAAATTTAAAG) and 2350C (CGCGGATCCCCATG-GTAATCCCAG) (the underlined bases correspond to the restriction sites for the *Sph*I and *Bam*HI restriction enzymes). The PCR product and the pQE70 vector (Qiagen, Valencia, CA) were digested with *Sph*I and *Bam*HI, and the linearized vector was dephosphorylated with shrimp alkaline phosphatase (Fermentas, Hanover, MD). The purified PCR product and vector were ligated and transformed into One Shot Top 10 competent cells, and plasmids containing the *cooSII* gene were isolated from ampicillin resistant colonies. The entire sequence of the *cooSII* gene and the immediate sequences upstream and downstream were confirmed by DNA sequencing. The resulting plasmid (pQECHIIHT) carrying the *cooSII* gene contains an additional Leu codon (CTA) at the N-terminus, four additional codons (GGA,

[1] Abbreviations: CODH-II, carbon monoxide dehydrogenase II; MES, 2-(*N*-morpholino)ethanesulfonic acid; Tris, 2-amino-2-(hydroxymethyl)-1,3-propanediol; HEPES, 4-(2-hydroxyethyl)-1-piperazineethanesulfonic acid; DTT, dithiothreitol; $CODH\text{-}II_{HT}$, recombinant CODH with a C-terminal six-His tag.

TCC, AGA, and TCT encoding Gly, Ser, Arg, and Ser, respectively), and a six-His tag (pQECHIIHT) at the C-terminus. This plasmid was transformed into *E. coli* BL21(DE3) Star containing the pRKISC plasmid (a generous gift from Y. Takahashi from Osaka University, Osaka, Japan), which carries the entire *ISC* operon from *E. coli*. Cells harboring both plasmids were recovered from Luria-Bertani plates containing ampicillin (0.1 mg/mL) and tetracycline (0.010 mg/mL). The recombinant strain was grown aerobically at 37 °C in a 2 L bottle containing 1 L of Terrific Broth continuously sparged with air. When the OD_{600} reached 0.6−0.8, the gas phase was switched to pure nitrogen for 30 min, and 0.1 mM $Fe(NH_4)_2(SO_4)_2$, 0.2 mM $NiCl_2$, 1.5 mM Na_2S, and 2.0 mM cysteine (final concentrations) were added. After 30 min, 0.2 mM isopropyl thiogalactoside was added to induce expression. After 15−17 h, the cells were harvested by centrifugation at 7000 rpm for 10 min at 4 °C. The cells were either stored at −78 °C for processing later or immediately lysed. Cells were lysed in a solution containing 50 mM potassium phosphate (pH 8.0), 10 mM β-mercaptoethanol, 0.3 M NaCl, and 10 mM imidazole (buffer A), supplemented with 0.2 mM phenylmethanesulfonyl fluoride, 0.25 mg/mL chicken egg lysozyme, and 4 units/mL deoxyribonuclease I. The suspension was sonicated for 6 min using 5 s pulses at 25% output. The homogenate was then centrifuged at 4 °C for 30 min at 30000 rpm and loaded onto a 1 cm × 5 cm Ni-nitrilotriacetate agarose column (Qiagen) in the anaerobic chamber. After extensive washing with buffer A, CODH-II_{HT} was eluted with buffer A supplemented with 240 mM imidazole. The fractions containing CODH-II_{HT} were pooled, dialyzed, and concentrated by ultrafiltration into 0.1 M Tris-HCl (pH 8.0) and 2 mM dithiothreitol. CODH-II_{HT} was judged to be >95% pure by SDS−PAGE. Peptide mapping by means of mass spectrometry analysis confirmed up to 70% of the protein sequence. The specific activities of the CODH-II_{HT} preparations were found to be between 200 and 400 units/mg at 30 °C, which is between 10 and 20%, respectively, of the native CODH-II from *C. hydrogenoformans.* Mutagenesis of pQECHIIHT was carried out using the QuickExchange kit from Stratagene. All mutations were confirmed by DNA sequencing of the entire *cooSII* gene.

NMR Spectroscopy and Samples. FT-NMR spectra were recorded in a Bruker Avance spectrometer operating at a ^{13}C frequency of 100.62 MHz with broadband proton decoupling. Samples in H_2O contain 10% D_2O for the internal field frequency lock. Samples in D_2O contained <10% H_2O. A total of 2560 transients were collected for 120 min with 32768 data points in the time domain, with a pulse acquisition delay of 2 s and a frequency window of 22075 Hz. For long time acquisitions, six blocks of 120 min were collected and averaged using the Bruker TopSpin software for a total of 15360 transients. The free induction decay data were processed with SpinWorks version 2.5.1 (K. Marat, 1999−2005, http://www.umanitoba.ca/chemistry/nmr/spinworks/) using a Fourier transformation with a zero filling function containing a total of 64K data points, a Lorentzian window function, and a line broadening of 1 Hz. The resonance peaks for ^{13}C-labeled CO, HCO_3^-, and CO_2 were observed at 184, 160, and 124 ppm, respectively. The pH-dependent resonance peak for $^{13}CN^-$ was observed within the range of 137−150 ppm (*33*). All frequencies are referenced to tetramethylsilane.

Table 1: Chemical Shifts, Line Widths, and Longitudinal Relaxation Times (T_1) for the Species Monitored in This Study

compound	chemical shift (ppm)	line width (Hz)	T_1 (s)
CO	184.2	0.36	2.70
$NaHCO_3$	160.2	2.44 (pD 7.0), 1.20 (pD 9.5)	24
CO_2	124.6	0.32 (pD 7.0), 0.02 (pD 9.0)	50
CN^-	137−150[a]	14.2	2.70

[a] The resonance of cyanide in solution is pH-dependent, and the reported position for CN^- in water is 165.7 ppm and for HCN 112.7 ppm. The observed range of parts per million corresponds to the pD range of 8.9−9.4.

The intensities of the peaks for the four species studied were calculated using the MES buffer peak integrations (0.1 M or 1 mM ^{13}C) as a reference. The concentrations of CO, CO_2, and $NaH^{13}CO_3$ were calculated from the integrated intensities applying a correction for the longitudinal relaxation times (T_1 values listed in Table 1). The T_1 values were measured by the usual inversion−recovery pulse sequence. The CO concentration was confirmed by injecting a small amount of the sample into an assay containing 2 mM sodium dithionite and 0.1 mM myoglobin (Calbiochem) and measuring the absorbance increase at 425 nm, using an extinction coefficient of 80000 M^{-1} cm^{-1}.

Line-shape analysis was carried out using Sigmaplot 5.0 (Systat Software, San Jose, CA). A four-parameter Lorentzian peak function (eq 2) was used for nonlinear regression.

$$y = y_o + \frac{a}{1 + \left(\frac{x - x_o}{b}\right)^2} \quad (2)$$

Four parameters were fit by the nonlinear regression analysis: the intensity offset, y_o; the intensity of the peak, a; the frequency offset for the resonance, x_o; and the half-width at the peak half-height, b. The validity of the fit was tested by fitting a Lorentzian peak prepared with a given set of parameters with eq 2 and by fitting the peak for CO obtained from spectra of the same sample but processed with different line broadening functions. The line broadening was calculated using eq 3, where $\Delta\upsilon$ is line broadening and υ_{CODH} and υ_o are the half-line widths at half-height for the peaks in the presence and absence of enzyme, respectively.

$$\Delta\upsilon = \upsilon_{CODH} - \upsilon_o \quad (3)$$

$$\text{rate}_{LB} = 2\pi\Delta\upsilon[S] \quad (4)$$

The exchange rate was calculated according to eq 4, which is only appropriate in the slow exchange limit. In this equation, [S] corresponds to the concentration of a species (CO, CO_2, HCO_3, or CN^-) obtained from the corresponding integrated intensity, after correction for T_1 with a time delay of 2.0 s. The pH or pD was confirmed by comparing the corresponding pL electrode reading with the ratio of concentrations of HCO_3^- and CO_2, based on a pK_a of 6.8 in D_2O.

For the ^{13}C isotope exchange experiments, the NMR samples were prepared in the anaerobic chamber by mixing buffer, D_2O, and CODH-II in a 1.5 mL Eppendorf tube and transferring the mixture to a 5 mm NMR tube from Norrell (Sigma-Aldrich), sealed with a 7 mm inside diameter rubber septum. After the sample had been flushed with ^{13}CO through a long 20 gauge Luer needle for 30−60 s, $NaH^{13}CO_3$ was injected from a 1 M stock solution. The solution was mixed

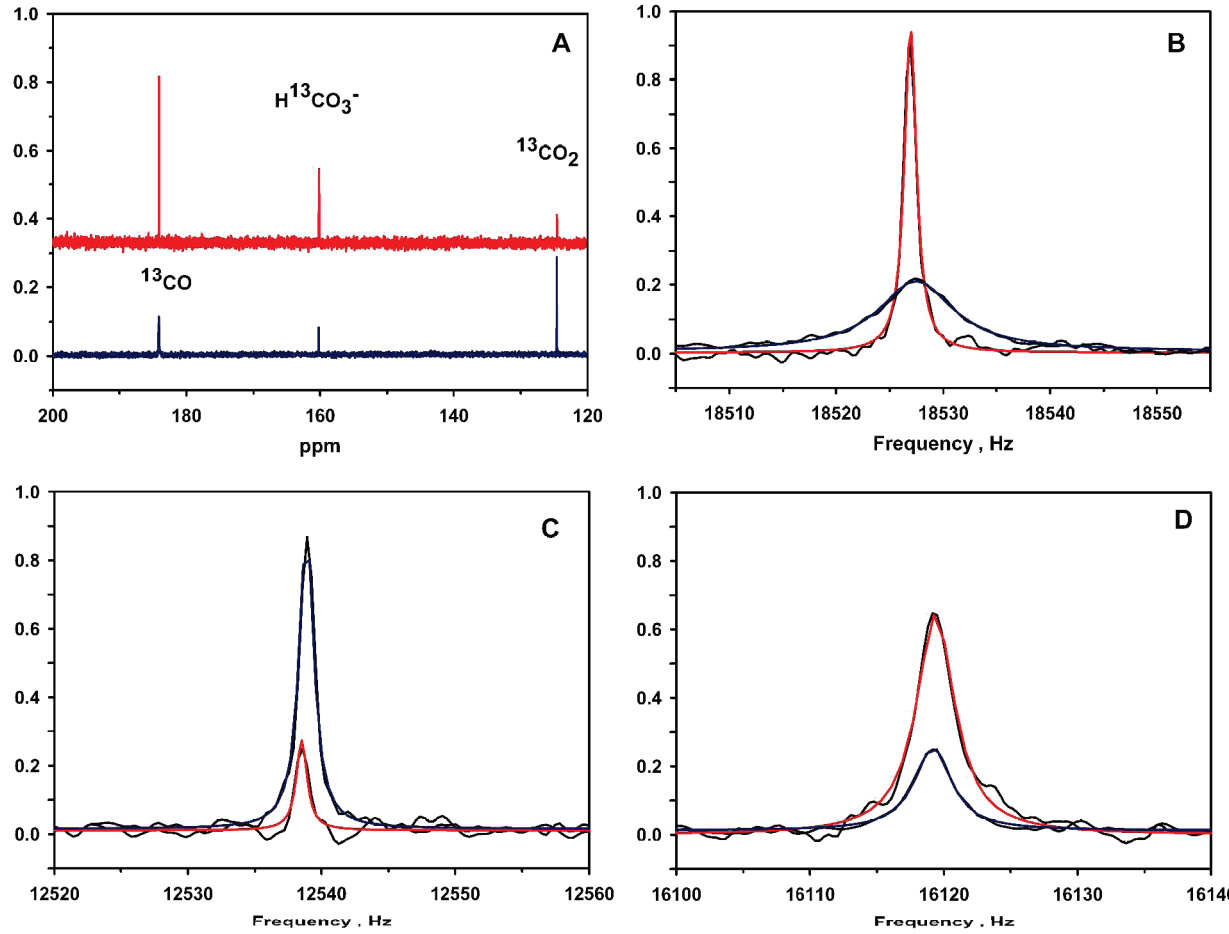

FIGURE 1: (A) ^{13}C NMR of an exchange reaction mixture containing 15 μM CODH-II (blue) or no CODH-II (red), 0.7 atm of ^{13}CO, and 5.0 mM $NaH^{13}CO_3$ in 0.1 M MES (pD 6.30) with >90% D_2O. MES buffer peaks are not shown. Spectra were collected for 12 h with decoupling of the proton channel. The concentrations as estimated from the T_1-corrected peak integrations are as follows: 0.7 mM ^{13}CO, 4.41 mM $^{13}CO_2$, and 1.31 mM $H^{13}CO_3^-$. (B) Fits to a four-parameter Lorentzian function of the ^{13}CO resonance peaks. Data without CODH-II show the fit in red and with CODH-II show the fit in blue. (C) Fits to a Lorentzian function of the $^{13}CO_2$ resonance peaks for the sample without CODH-II (red fit) and with CODH-II (blue fit). (D) Fits to a Lorentzian function of the $H^{13}CO_3^-$ resonance peaks for the sample without CODH-II (red fit) and with CODH-II (blue fit). NMR peak intensities are normalized for clarity.

at room temperature and allowed to reach equilibrium for 60−90 min prior to the commencement of data acquisition. That the samples were poised at equilibrium was confirmed by recording six 2 h spectra in 12 h. A <5% variation in the intensities of each of the peaks was observed.

For the NMR isotope exchange experiments, the samples were prepared in the anaerobic chamber as just described except that they were flushed with 100% unenriched CO for 10 min before 50 mM $NaH^{13}CO_3$ was added. Shortly before the initiation of data acquisition, a small aliquot of CODH-II stock was injected. The time interval between the injection of the enzyme (between 4 and 5 min) and the half-point of the first spectrum (~19 min) was taken as the first time point. For the remainder of the time acquisition, the time for each point was generated by adding 38 min. The integration of the ^{13}CO peak was corrected for T_1 with a time delay of 2.0 s and plotted versus time. The plots were then fitted to eq 5, the exponential form of the isotope exchange equation:

$$[^{13}CO] = [^{13}CO_{inf}][1 - \exp(\mathrm{vel} \times t/[CO])] \qquad (5)$$

where $[^{13}CO_{inf}]$ is the concentration at infinite time, [CO] is the total constant concentration of CO, and vel is the rate of isotopic exchange under conditions where $[CO_2] \gg [CO]$.

RESULTS

^{13}CO Exchange Broadening. Upon addition of CODH-II to a solution containing ^{13}CO and $^{13}CO_2$, the ^{13}CO resonance exhibits significant broadening (Figure 1A,B). The observed $\Delta\upsilon_{CO}$ values were in the range between 1 and 30 Hz, depending on the conditions. To compare the results to normal steady-state conditions for CO oxidation, the concentrations of the substrates were at least 10-fold higher than that of CODH-II. As shown in Figure 1, when the solution contained 0.7 atm (0.69 mM) of ^{13}CO and 5.0 mM $NaH^{13}CO_3$, the observed line widths for ^{13}CO, $^{13}CO_2$, and $H^{13}CO_3^-$ were 0.68, 0.63, and 1.73 Hz, respectively, without enzyme, as obtained from fits to eq 2. In the presence of 15 μM CODH-II, the resonances "broadened" to 4.32, 0.66, and 1.66 Hz, respectively, yielding line broadenings for ^{13}CO, $^{13}CO_2$, and $H^{13}CO_3^-$ of 3.64, 0.03, and −0.07 Hz, respectively. The broadening values for $^{13}CO_2$ and $H^{13}CO_3^-$ are insignificant, given the error of the measurement, since line broadening values in the range of 0.5 Hz can originate from slight discrepancies in the tuning of the broadband probe of the instrument. Furthermore, there was no consistent dependence of the CO_2 line width broadening on the CO_2 or CODH-II concentration. The T_1-corrected integrations for the

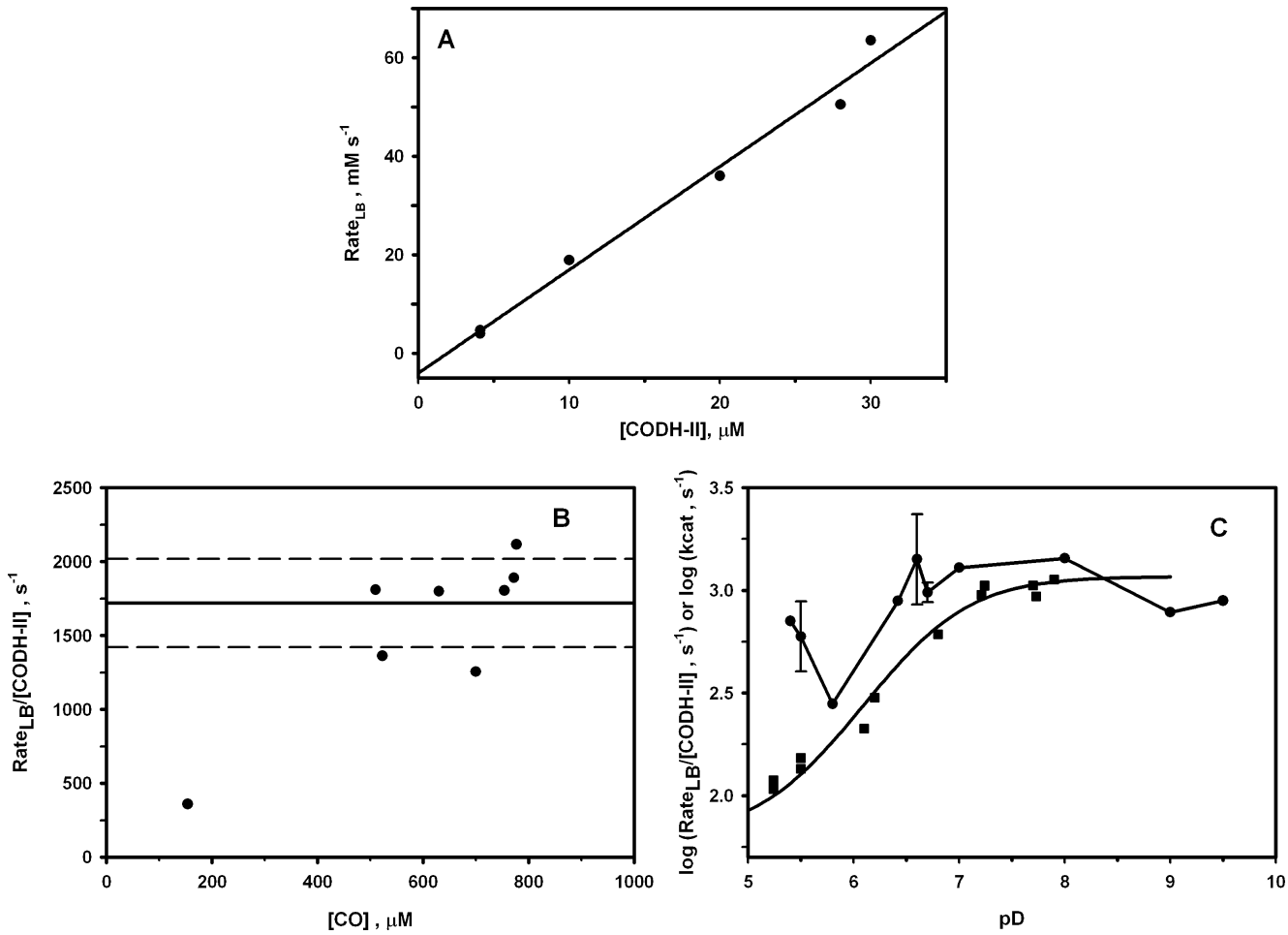

FIGURE 2: (A) Dependence of the broadening exchange rate ($rate_{LB}$) on the CODH-II monomer concentration. Other conditions are 0.5−0.7 atm of ^{13}CO, 50 mM $NaH^{13}CO_3$, and 0.1 M MES (pD 6.8). The T_1-corrected integrations of the ^{13}CO peak were used to calculate the ^{13}CO concentrations. The slope of the linear regression is 2000 ± 200 s^{-1}. (B) Dependence of $rate_{LB}$ after normalization for CODH-II concentration on the CO concentration. The line at 1700 s^{-1} represents the average of all the measurements shown, while the dashed lines indicate the standard error (300 s^{-1}). (C) Effect of pD on the exchange broadening for the CO resonance (●) and pH dependence of k_{cat} for CO oxidation (■). The steady-state measurements were carried out at 20 °C, in 20 mM methyl viologen, 1 atm of CO, and 0.1 M MES buffer.

resonances were used to calculate the concentrations of ^{13}CO, $^{13}CO_2$, and $H^{13}CO_3^-$ in the reaction mixture, which were 0.71, 4.41, and 1.31 mM, respectively.

To ensure that the exchange process is in the slow exchange limit, we performed the experiment at varying concentrations of CODH-II. Although the amount of CO broadening is proportional to the CODH-II concentration (Figure 2A), the ^{13}CO, as well as the HCO_3^- and CO_2, chemical shifts were unchanged by addition of CODH-II (Figure 1B−D), and reproducible within 0.1 Hz for different experiments. Under the slow exchange regime of the NMR time scale, the exchange process can be expected to affect the line widths of the exchanging resonances and not the resonant frequencies or the longitudinal relaxation rate constants ($1/T_1$ values). Therefore, the ^{13}CO chemical exchange occurs at a much slower rate than the time scale of acquisition of the NMR spectra, i.e., $2\pi\Delta\omega$, where $\Delta\omega$ is the resonance frequency difference between the exchanging species. For a slow exchange process, $2\pi\Delta\omega^*/\Delta\upsilon \gg 1$ (*25*), where $\Delta\upsilon$ is the line broadening, as defined in Materials and Methods. For a chemical exchange between CO and CO_2, $\Delta\omega$ (i.e., $\omega CO - \omega CO_2$) = 60 ppm or 6000 Hz; thus, $2\pi\Delta\omega$ equals approximately 36000 s^{-1}. Likewise, for the exchange between CO and HCO_3^-, Δ = 23 ppm or 2300 Hz. Thus, both of the resonance frequency differences are much larger than the maximum observed broadening for CO of ∼30 Hz. That the CO resonance exhibits line broadening but remains at the same chemical shift as free CO demonstrates conclusively that the ^{13}CO chemical exchange process is within the slow exchange limit of the NMR experiment. Under this time regime, eq 3 is the appropriate treatment for the broadening ($\Delta\upsilon$), and the ^{13}CO line broadening is expected to be proportional to the exchange rate as shown by eq 4. According to eq 4, the rate of the ^{13}CO chemical exchange is 16.8 mM s^{-1}. This value equates to a rate constant of 1080 s^{-1} at 20 °C, based on a monomeric unit of CODH-II. The exchange rate ($rate_{LB}$) in turn is proportional to the enzyme concentration, as shown in Figure 2A.

We were unable to observe the expected dependence on CO concentration (Figure 2B). The likely reason is that the low K_m value for CO in the CO oxidation reaction catalyzed by CODH-II (18 μM) (*2*) is well below the lowest CO concentration that could be used in these experiments (0.2 mM). This is because the ^{13}CO signal could not be observed at concentrations of <0.1 mM ^{13}CO due to the inherent insensitivity of the NMR method and the long T_1 value for

CO (2.7 s) (Table 1).[2] Similarly, the $^{13}CO_2$ signal was not observed at concentrations of <0.5 mM $^{13}CO_2$. T_1 values were measured by the standard inversion−recovery method in the absence of enzyme. Since the K_m value for CO is well below the NMR detection threshold and since there is no observable dependence of the line width on CO concentration, it is reasonable to conclude that the broadening exchange rates are values at saturation. Therefore, the $rate_{LB}$/[CODH] constants are directly comparable to k_{cat} values for CO oxidation, CO_2 reduction, and the isotopic exchange rate constant.

The ^{13}CO line broadening could arise from any exchange process involving free CO and a form of CO or CO_2 with an inherently different chemical shift as long as it is on the reaction pathway, i.e., bound CO, or bound or free CO_2 (or perhaps bicarbonate). If the ^{13}CO line broadening were to originate from an exchange between ^{13}CO and $^{13}CO_2$ (or $H^{13}CO_3^-$) in solution, one would expect to observe a line broadening for both of these resonances, as described in eq 6, which was derived for the $^{13}CO_2-H^{13}CO_3$ exchange catalyzed by carbonic anhydrase (*26*).

$$2\pi\Delta\upsilon_{[CO]}[CO] = 2\pi\Delta\upsilon_{[CO_2]}[CO_2] \quad (6)$$

Specifically, for the CODH-II reaction, if the CO and CO_2 concentrations are equivalent, the amount of broadening of the $^{13}CO_2$ (or $H^{13}CO_3^-$) resonance should equal that of the ^{13}CO resonance. In most experiments, the CO concentration was in the range of 0.5−1.0 mM and the combined concentrations of CO_2 and bicarbonate ranged from 0.5 to 50 mM. However, as noted above, only the ^{13}CO resonance exhibits significant broadening upon addition of CODH-II (blue line in the presence of CODH-II, red line in its absence) with a $\Delta\upsilon$ of 3.64 Hz and a $rate_{LB}$ of 16.8 mM s^{-1} (Figure 1B−D). With 5.0 mM $^{13}CO_2$ and CODH-II concentrations as high as 0.05 mM, no significant broadening of the $^{13}CO_2$ or $H^{13}CO_3^-$ resonances could be detected.[3] Furthermore, broadening was not observed for the $^{13}CO_2$ resonance even at a concentration of 250 μM CODH-II (monomer), in the absence of CO, or in the presence of the reductant sodium dithionite at 2 mM (in the absence of CO). In addition, when the pD of the reaction was lowered (to decrease the bicarbonate concentration) or when the CO_2 concentration was decreased at a constant CO concentration, broadening of $^{13}CO_2$ resonance was not observed. These results clearly indicate that exchange between free CO and free CO_2 in solution is not responsible for broadening of the ^{13}CO resonance and suggest that this process originates from an exchange reaction involving CO and some bound form of CO or CO_2 but does not include the final step, release of CO_2 into solution. Further support for this view comes from the lack of an effect of the CO_2 concentration on the ^{13}CO broadening, indicating that free CO_2 is not in equilibrium with bound CO, bound CO_2, or free CO along the exchange pathway responsible for the broadening. Moreover, CO_2 and bicarbonate are at chemical equilibrium, as their ratio was found to be invariant over the time of the experiments (2 h) and this ratio was quite close to the value calculated from the pK_a for CO_2 (6.80 in D_2O). Although the $CO_2/H^{13}CO_3^-$ ratio does vary with the pH, it does not affect the broadening of ^{13}CO (Figure 2C). A different approach, described below, for studying the exchange reaction between CO and CO_2 in solution reveals that this reaction occurs nearly 3 orders of magnitude more slowly than the ^{13}CO line broadening.

Broadening of the bicarbonate resonance was observed at pD >8.0. The extent of broadening was similar to that of the ^{13}CO resonance, but given the high concentrations of bicarbonate which accumulated at high pD (measured directly in the NMR experiment to be >50 mM), the resulting exchange rates are ~100 times higher than those for CO. Since CO_2, not bicarbonate, has been shown to be the product of the CODH reaction, observation of line broadening with bicarbonate and not CO_2 suggests that $H^{13}CO_3^-$ line broadening does not involve any step in CO oxidation. The extent of broadening of bicarbonate was significantly reduced at higher MES buffer concentrations (not shown), suggesting that the $H^{13}CO_3^-$ broadening is likely to come from general base catalysis of CO oxidation. This was confirmed by measuring the stimulating effect of bicarbonate on the CO oxidation activity under steady-state conditions in the absence of buffer (Supplementary Figure 1) and by the fact that bicarbonate broadening was not observed in the absence of CO or CODH-II. Thus, broadening of the $H^{13}CO_3^-$ resonance under these conditions must result from binding and dissociation of bicarbonate from some anion binding site on CODH and not from a CO−bicarbonate exchange reaction. Although $H^{13}CO_3^-$ line broadening is an interesting phenomenon, our studies focused on characterization of the ^{13}CO line broadening, which clearly involves steps included in the CO oxidation reaction.

The results described above indicate that the ^{13}CO line broadening originates from an exchange between CO and some CODH-bound form of CO or CO_2 with a chemical shift that is different from that of free ^{13}CO. The line broadening is truly an exchange process and does not result simply from immobilization of CO or CO_2 within the protein because, if ^{13}CO were firmly immobilized on the CODH homodimer (molecular mass of ~130 kDa), the rotational correlation time of the complex would equal that of the protein, which is ~56 ns.[4] On the basis of this correlation time, a simple calculation of the transverse relaxation rate (T_2) yields a value of ~0.29 s (*34*), which would contribute a ^{13}CO line width broadening $\Delta\upsilon$ of only 1.1 Hz. Another consideration is that, since CODH is a metalloenzyme, one might suspect that the broadening might come simply from a paramagnetic effect, e.g., binding of CO to a paramagnetic C-cluster. However, even though a ^{13}C resonance near a paramagnetic metal center would certainly experience para-

[2] Because of the high T_1 values, with 100 μM ^{13}CO, a 50 μM ^{13}C peak can be observed; with 500 μM $^{13}CO_2$, only an 20 μM ^{13}C peak can be observed.

[3] The rate constants (k_{cat} values) for CO and CO_2 broadening are the numbers for the rates divided by the CODH-II concentration, 15 μM. For CO, it is 16.8/0.015 = 1120 s^{-1}, and for CO_2, it would be 0.83/0.015 = 55 s^{-1}. Thus, it is clear that CO and CO_2 (in solution) are not exchanging. Moreover, no effect of the $^{13}CO_2$ and $H^{13}CO_3^-$ concentrations on the broadening of the ^{13}CO resonance was observed, consistent with the lack of involvement of these two species in the ^{13}CO broadening.

[4] The rotational correlation time was estimated as the molecular mass divided by 2400 ns, assuming a globular protein with spherical symmetry. T_2 was calculated by a simple relationship derived from the Bloembergen−Purcell−Pound theory of nuclear magnetic relaxation (*1*).

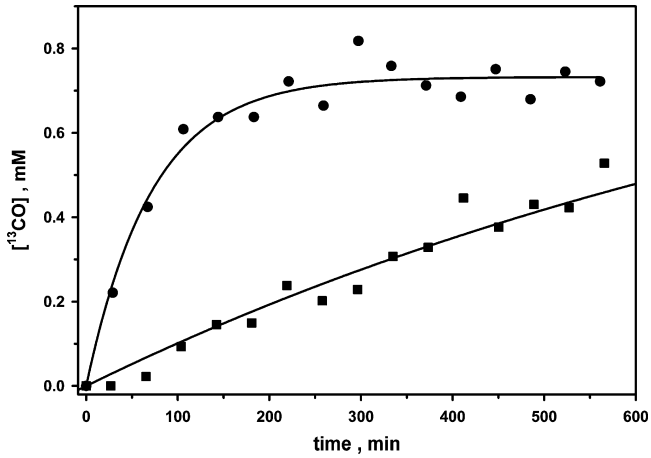

FIGURE 3: Isotope exchange at equilibrium between CO and $^{13}CO_2$/$NaH^{13}CO_3$. The samples were prepared and the spectra recorded as indicated in Materials and Methods. The two assays contained 90 (●) and 9 nM (■) CODH-II monomers. The amplitudes and rate constants for these assays were 0.70 mM and 0.0139 min^{-1} (●) and 1.0 mM and 0.001 min^{-1} (■), respectively. The data were fit according to eq 5 shown in the text. The concentrations of CO and $^{13}CO_2$/$H^{13}CO_3$ were 0.7 atm and 50 mM, respectively.

magnetic broadening (and, if it were directly bound, it would also shift markedly in frequency), the broadening of the free CO resonance under the slow exchange regime with respect to the NMR time scale depends on the rate of exchange, but not on the line widths of the bound ^{13}CO or bound $^{13}CO_2$ resonance. Therefore, the bound form of CO or CO_2 may be paramagnetic or diamagnetic, but a paramagnetic effect is not responsible for the observed ^{13}CO line broadening. We also show (vide infra) that a functional C-cluster, which is the active site for CO oxidation and CO_2 reduction, is required for observation of any significant ^{13}CO line broadening, also indicating that broadening does not originate from simple binding and release of CO from CODH-II.

Isotope Exchange between CO and $^{13}CO_2$. To improve our understanding of the origin of the CO line broadening, we measured the isotopic exchange between CO and CO_2 in solution by following the incorporation of ^{13}C from $^{13}CO_2$ into ^{13}CO in the presence of ^{12}CO at lower concentrations of enzyme (<1 μM) than in the CO line broadening experiments. Under these conditions, broadening of the ^{13}CO resonance was not noticeable. Since the concentrations of the substrates are much higher than that of enzyme, the assay is expected to follow the steady-state kinetics of isotope exchange at chemical equilibrium. The number of averaged transients was reduced to 768 scans per spectrum with 8192 data points (38 min collection time per spectrum) in the time domain for detection of the incorporation of ^{13}C into CO. The amount of ^{13}CO increased exponentially with time, as expected for a first-order exchange process, with an amplitude equivalent to the total CO concentration and with a k_{exc} (vel/[CODH]) of ~1.7 s^{-1}, calculated according to eq 5 (Figure 3). The total concentrations of CO (~0.7 atm), $^{13}CO_2$, and $H^{13}CO_3^-$ (50 mM) did not change during the experiment, as determined from the T_1-corrected peak integrations, indicating that an isotope exchange had occurred at equilibrium in which ^{13}C from $^{13}CO_2$ was incorporated into CO. The isotope exchange rate (vel) was found to be proportional to the CODH concentration (not shown). To compare this isotope exchange reaction with the steady-state initial velocity of CO_2 reduction, the reduction of CO_2 to CO was assessed at 20 °C by following the formation of Mb-CO (*35*) with 2 mM sodium dithionite as the reductant, yielding a K_{mCO_2} of 0.5 mM and a k_{cat} of 2 s^{-1} (Supplementary Figure 2). In contrast, the steady-state parameters for CO oxidation by CODH-II are as follows: K_{mCO} = 18 μM, K_{mMV} = 4 mM, and k_{cat} = 15900 s^{-1} per monomer at 70 °C (*2*). At 20 °C, the k_{cat} for CO oxidation decreases to 1500 s^{-1}, while the K_m values for the substrates are temperature-independent. Thus, for the isotope exchange between CO and CO_2 in solution (k_{cat} = 1.7 s^{-1}), the reduction of free $^{13}CO_2$ to ^{13}CO is rate-limiting (k_{cat} = 2 s^{-1}), as this step is 750-fold slower than CO oxidation. Since the rate constant for ^{13}CO line broadening (1080 s^{-1} at 20 °C) is comparable to that for CO oxidation (k_{cat} = 1500 s^{-1} at 20 °C), the steps involved in ^{13}CO exchange broadening could include CO binding and oxidation to a bound form of CO_2, followed by conversion of bound CO_2 back to bound CO and re-release of CO into solution. However, one can clearly rule out the possibility that the ^{13}CO line broadening includes the release of CO_2 from the enzyme and the reduction of solution CO_2 back to CO, since these steps occur too slowly to be part of the ^{13}CO exchange process and, as described above, only ^{13}CO (and not $^{13}CO_2$) line broadening is observed. These results also suggest that the equilibrium between the CO_2/CO and CODH-II_{ox}/CODH-II_{red} redox couples (eq 7), the "ping" phase of this ping-pong reaction, is significantly shifted to the right.

$$CO + H_2O + CODH_{ox} \leftrightarrow CODH_{red} + CO_2 + 2H^+ \quad (7)$$

Properties of the Exchange Broadening of ^{13}CO. As described above, the slow rate of the exchange reaction between free CO and free CO_2 (~500 times slower than the ^{13}CO exchange broadening) and the lack of $^{13}CO_2$ line broadening clearly show that an exchange between CO and solution CO_2 is not part of the ^{13}CO line broadening mechanism. Thus, we performed NMR experiments using site-directed mutants of CODH to distinguish whether the chemical exchange reaction responsible for the ^{13}CO line broadening involves only binding and release of CO or if it also includes the formation of bound CO_2 and its reduction back to bound CO.

We considered the possibility of a collision broadening mechanism without conversion of CO into CO_2 by CODH-II. This could occur by simple binding of CO to CODH and release of CO back into solution. To test this possibility, we assessed the ^{13}CO exchange with two site-directed variants of recombinant CODH-II (CODH-II_{HT}): K563L, which is an acid−base variant that is compromised in generating CO_2 from CO (*36*), and C56A, which lacks a functional B-cluster, allowing it to generate CO_2 but disabling electron transfer to external redox mediators. The C56A variant was devoid of CO oxidation activity (as measured by viologen reduction), yet it exhibited a ^{13}CO broadening of 40 s^{-1} (Table 2). Besides lacking a functional B-cluster, this variant exhibits ~10% of the amount of C-cluster found in native CODH-II. If one corrects for the amount of C-cluster, the ^{13}CO line broadening is expected to be ~400 s^{-1}, which is only ~3-fold lower than that observed for the native protein under these conditions. Therefore, although a functional B-cluster

Table 2: Summary of Line Broadenings and $rate_{LB}$ Values for the ^{13}CO Peak for CODH-II and Its Variants[a]

	$\Delta\nu$ (Hz)	[CODH-II] (μM)	$rate_{LB}$/[CODH-II] (s^{-1})
CODH-II, 0.1 M MES, 4.0 mM $NaHCO_3$	9.17	25.2	1600 ± 20
CODH-II, no buffer, 50 mM $NaHCO_3$	3.97	15.0	1160 ± 30
CODH-II, 0.1 M MES, 50 mM $NaHCO_3$	4.70	15.0	1380 ± 30
CODH-II, 0.9 M MES, 5.0 mM $NaHCO_3$	5.60	15.0	1640 ± 30
Ni-depleted $CODH\text{-}II_{HT}$	<0.01	14.2	3.1
K563L $CODH\text{-}II_{HT}$	<0.01	11.0	4.0
C56A $CODH\text{-}II_{HT}$	0.45	46.8	42 ± 9
A571W $CODH\text{-}II_{HT}$	0.20	8.8	100 ± 50

[a] Conditions are >90% D_2O, 0.7 atm of ^{13}CO, 5.0 mM $NaHCO_3$, and 0.1 M MES (pD 7.0) at 20 °C, unless indicated otherwise. The standard errors in the broadening are estimated to be 0.1 Hz.

is required for electron transfer to viologens, it is not required in the reaction steps involved in line broadening of ^{13}CO.

The K563L variant, which is an acid−base mutant that is compromised in the elementary steps leading to CO_2 formation, has very low CO oxidation activity (0.6 unit/mg; k_{cat} = 0.67 s^{-1}); furthermore, it exhibits no observable CO broadening. An extensive kinetic characterization of this variant will be reported separately, but it suffices for this experiment to conclude that the conversion of CO to CO_2 is necessary for the observation of ^{13}CO line broadening.

We expressed $CODH\text{-}II_{HT}$ in the absence of Ni^{2+} ions to generate the *C. hydrogenoformans* enzyme with a C-cluster that is depleted in the nickel site (~0.1 Ni/monomer) but contains the B- and D-clusters and the FeS component of the C-cluster (~9 Fe/monomer). Similar properties were reported for a Ni-depleted CODH from *R. rubrum* (*37*). As with the *R. rubrum* enzyme, the Ni-depleted *C. hydrogenoformans* enzyme has very low CO oxidation activity (k_{cat} = 10 s^{-1}). Furthermore, it exhibited no observable ^{13}CO line broadening (Table 2).

The combined results of these experiments indicate that a functional C-cluster and the ability to oxidize CO to CO_2 are required for ^{13}CO exchange broadening (as well as CO oxidation activity), but B-clusters are not. Thus, the mechanism of CO broadening must involve binding of CO to and release of CO from CODH-II, and CO oxidation to bound CO_2. However, electron transfer through the B- and D-clusters is not required for ^{13}CO line broadening. Furthermore, the lack of $^{13}CO_2$ line broadening demonstrates that during this exchange reaction, the CO_2 is not released into solution but remains bound to the enzyme, as shown in eq 8.

$$CO + H_2O + CODH_{ox} \leftrightarrow CODH_{ox} - CO - H_2O \leftrightarrow CODH_{red} - CO_2 - 2H^+ \quad (8)$$

Surprisingly, the ^{13}CO line broadening is independent of pH, remaining within the range between 560 and 1200 s^{-1} over the pD range from 5.5 to 9.0 (Figure 2C).[5] In sharp contrast, the steady-state rate of CO oxidation measured by following reduction of an external electron acceptor (20 mM methyl viologen) at the same temperature (20 °C) increases with pH, according to a pK_a of 6.70 and a k_{max} of 1160 s^{-1} (Figure 2C). This result indicates that protons equilibrate with solvent during the steady-state reaction but protons are not released into solution during the ^{13}CO exchange reaction, as shown by eq 8. A similar difference between the exchange reaction and the steady-state reaction was observed for carbonic anhydrase, as described in the introductory section.

Table 3: Summary of Line Broadenings and $rate_{LB}$ Values for the $^{13}CN^-$ Peak for CODH-II and Its Variants[a]

	$\Delta\nu$ (Hz)	[CODH-II] (μM)	C_{red2} per CODH-II	$rate_{LB}$/[CODH-II] (s^{-1})
native $CODH\text{-}II$[b]	20 ± 0.5	15	0.5	33500 ± 1000
Ni-depleted $CODH\text{-}II_{HT}$	3.6 ± 0.10	28	<0.1	4040 ± 110
K563L $CODH\text{-}II_{HT}$	0.70 ± 0.02	36.5	<0.1	600 ± 20

[a] Conditions are >90% D_2O, 5.0 mM $K^{13}CN$, 5.0 mM $NaHCO_3$, and 0.1 M MES (pD 7.0) at 20 °C. [b] This sample had 4.0 mM $K^{13}CN$.

Exchange Broadening of Cyanide. To improve our understanding of the origin of ^{13}CO exchange broadening, we studied the interaction of CODH-II with $^{13}CN^-$, which binds to CODH but does not undergo oxidation. Potassium cyanide is a strong competitive inhibitor of the CO oxidation reaction (*38*), although with some CODHs, CN^- binding can be rather complex (*39, 40*). Addition of 5 mM $K^{13}CN$ in the presence of HCO_3^-, and in the absence of CO, leads to a marked broadening of the $^{13}CN^-$ resonance, which yields a rate of exchange between free and CODH-II-bound CN^- of 33500 s^{-1} (Table 3), which is ~30-fold higher than the rate of ^{13}CO exchange broadening. No observable broadening of the resonances for $^{13}CO_2$ and $H^{13}CO_3^-$ was observed in samples in which CODH-II was incubated with $K^{13}CN$ and $NaH^{13}CO_3$. Under the conditions of these experiments, CODH-II should be saturated with cyanide (K_i = 21 μM) (*38*); correspondingly, the NMR samples prepared with $K^{13}CN$ showed no detectable CO oxidation activity, indicating complete inhibition of CODH activity by CN^-. CO can relieve inhibition by CN^- (*40*), and indeed, the magnitude of broadening of the $^{13}CN^-$ resonance decreased by ~2-fold to 19000 s^{-1} in the presence of 0.7 mM CO. Accordingly, magnitude of broadening of the ^{13}CO resonance was reduced from ~1120 to 370 s^{-1} in the presence of 5.0 mM $^{13}CN^-$. Similarly, in the steady-state reaction, when CODH-II was exposed to CO, MV, and 5 mM KCN, the k_{cat} for CO oxidation decreased by 50%, indicating that the K_i values for CO and CN^- are similar and that CO and CN^- compete at the CODH active site. These results also are consistent with the view that the reactions responsible for CO exchange broadening are on the pathway of CO oxidation and that CN^- interferes with this process. They are also consistent with free $^{13}CO_2$ not being a component of the broadening exchange pathway for either CO or CN^-.

Cyanide has been proposed to bind to the Ni (*37–39*) or the Fe1 subsites (*41*) of the C-cluster. Since cyanide is not

[5] When the pD dependence was fitted with increasing pD with the inclusion of error bars, a k_{max} of 1100 ± 600 s^{-1} and pK_a of 5.4 ± 1.1 were obtained. Given the large standard error for this fit and the large discrepancy between the calculated pK_a for the exchange (5.4) and the value obtained for the CO oxidation reaction (6.7), we conclude that the exchange reaction is pH-independent. A likely explanation for a slight decrease in the level of exchange broadening when the pD is lowered to 6.0 and an increase at even lower pH values is that the conversion of $CODH_{red}$−CO_2 to $CODH_{ox}$−CO becomes rate-limiting at low pH and requires protonation of CO_2 as the first step in the formation of water. Since CODH-II precipitates at pD below ~5.0, the entire pD profile could not be accurately measured.

oxidized by CODH-II, the last step of eq 8 does not occur, which provides an explanation for the exchange rates being higher for CN^- than for CO. Thus, $^{13}CN^-$ broadening likely involves only binding of CN^- to and release of CN^- from CODH. The level of broadening of $^{13}CN^-$ was depressed to a much smaller extent than the level of broadening of CO upon Ni depletion of CODH-II_{HT} (Table 3), implying that a fully functional C-cluster is not required for the exchange broadening of cyanide. Since Fe in the C-cluster is not deficient in the Ni-depleted enzyme, one explanation for these results is that CN^- may bind to Fe, not Ni. Another possibility, discussed below, is that CN^-, a slow binding inhibitor (*39, 42*), may bind in two phases. The $^{13}CN^-$ broadening was still observed with the K563L mutant, although the level of broadening is reduced more than for the Ni-deficient enzyme, perhaps due to an electrostatic effect of the amino group of Lys-563 on CN^- binding.

DISCUSSION

The NMR studies described here provide novel information about the enzymatic oxidation of CO to CO_2 by focusing on three CODH-catalyzed reactions: (1) a ^{13}CO chemical exchange, which involves broadening of the ^{13}CO NMR resonance, (2) a relatively slow exchange between ^{13}CO and solution $^{13}CO_2$, and (3) a $^{13}CN^-$ chemical exchange. The ^{13}CO line broadening and the $^{13}CO-{}^{13}CO_2$ exchange focus on the chemical steps of CO oxidation and an associated proton transfer reaction, while the $^{13}CN^-$ exchange is considered to reflect movement of CO through a proposed CO channel. These studies used native CODH-II, recombinant wild-type CODH-II_{HT}, and variants of the recombinant protein that are compromised in different steps in the CO oxidation mechanism. Development of a method for following the chemistry of CO oxidation is important because this reaction occurs too fast for most transient kinetic methods, like stopped-flow or rapid freeze-quench EPR [though a recently developed freeze quenching method (*43*) may be feasible]. The use of this NMR-based ^{13}CO exchange in the absence of electron carriers also ensures that the chemistry of CO oxidation is followed, not electron transfer, which is rate-limiting under some conditions (*19*). Assessment of the carbonic anhydrase-catalyzed $^{13}CO_2-H^{13}CO_3^-$ exchange reaction provided the inspiration and the theoretical background for this series of experiments (*23–26*).

As shown in Figure 4, CO oxidation involves CO binding to the C-cluster, CO oxidation to bound CO_2, release of protons and CO_2 to solution, and electron transfer to the B- and D-clusters, which transfer electrons to external redox mediators. This scheme is similar to one proposed in a recent structural paper in which bound CO_2 was trapped as a bridging ligand between Ni and an asymmetrically coordinated Fe, which has been called Fe1 (also called ferrous component II, FCII) (*9*). Another proposed step in the CO oxidation reaction based on the X-ray structure of dithionite-reduced CODH-II involves channeling of CO and water from the surface to the C-cluster (*14*). CO is proposed to migrate through a hydrophobic channel, and water molecules are proposed to move through a hydrophilic channel. Thus, NMR-detected chemical exchange reactions involving ^{13}CO or competitive inhibitor $^{13}CN^-$ would include entry of the free species at the mouth of the CO channel and migration to the C-cluster.

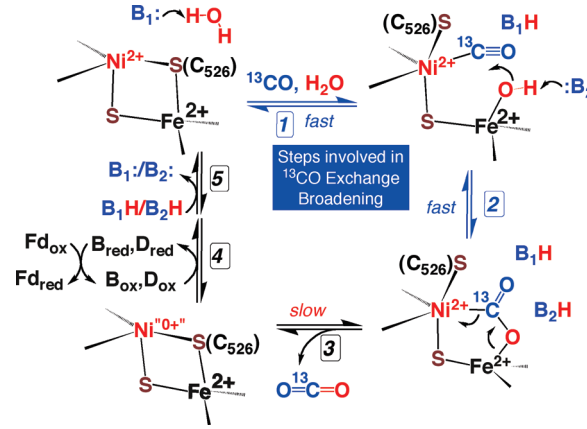

FIGURE 4: Revised mechanism of CO oxidation suggested by ^{13}C NMR experiments. Steps 1 and 2, which are monitored by the ^{13}CO line broadening experiments, are designated with blue arrows. Exchange of bound $^{13}CO_2$ with solution CO_2 is too slow to be involved in ^{13}CO exchange broadening.

CODH-II was found to catalyze a ^{13}CO chemical exchange reaction, which occurs with a rate constant that approximates the k_{cat} for CO oxidation and is within the slow exchange limit of the NMR experiment. We have considered the broadening effect due to simple CO and CN^- binding to CODH and release from CODH in the slow exchange regime. Although ligand binding to a macromolecule is expected to produce some degree of broadening of the resonance for the free ligand, this behavior is usually observed when the experiment is performed in titration mode; that is, the ratio of ligand to binding sites is not higher than 10-fold. The corresponding equations for the broadening of the free (L) and bound (ML) forms of a ligand in a 1:1 stoichiometric complex (ML) (which should have a chemical shift different from that of L) are as follows:

$$2\pi(\Delta\upsilon_L)_{obs} = \left(\frac{1}{T_{2L}}\right)_{obs} - \frac{1}{T_{2L}} = k_{-1}\frac{f_{ML}}{f_L} \quad (9)$$

$$2\pi(\Delta\upsilon_{ML})_{obs} = \left(\frac{1}{T_{2ML}}\right)_{obs} - \frac{1}{T_{2ML}} = k_{-1} \quad (10)$$

In these equations, T_{2L} and T_{2ML} are the transversal relaxation times for free (L) and bound (ML) ligand, respectively, k_{-1} is the constant for dissociation of L from the ML complex, and f_{ML} and f_L are the fractions of ligand in the bound and free states, respectively. The broadening of the bound form ($2\pi\Delta\upsilon_{ML}$) depends only on the chemical exchange rate constant for the dissociation (k_{-1}), whereas that of the free form ($2\pi\Delta\upsilon_L$) depends on the saturation fraction. Under the conditions of our experiments, 300 μM < [CO] < 1000 μM and [CODH-II] ~ 15 μM, which means that f_{ML}/f_L varies between 0.052 and 0.015. If $k_{-1} \sim 1000\ s^{-1}$ at 20 °C (the value of k_{cat} for CO oxidation at this temperature), a broadening between 2.4 and 8 Hz would be expected for the free CO (L) resonance and a broadening of ~160 Hz [$k_{-1}/(2\pi)$] would be expected for the bound resonance (ML). If bound CO was rapidly converted to bound CO_2, a similar broadening of ~160 Hz would be expected. These numbers are consistent with the observed broadenings for native CODH (4−9 Hz). Therefore, the NMR experiments are consistent with a process involving chemical exchange between free CO and bound ligand; however, these experiments cannot alone distinguish between whether the chemical

exchange is between free CO and bound CO or bound CO_2. On the other hand, the NMR experiments clearly rule out the involvement of free CO_2 in the exchange process, because no increase in the line width of the free CO_2 resonance is observed.

Thus, in a chemical exchange between free CO and either bound CO or bound CO_2, the line width of the bound ligand is predicted to be very broad, probably too broad to observe. To confirm that the broadening includes chemistry at the CODH active site and does not just reflect binding and release of CO, we compared activities of several CODH variants. The recombinant enzyme exhibits 10−20% of the activity and contains 10−20% of the Ni present in the native protein. The extent of line broadening is also 10−20% of that observed with the native protein, indicating (as expected) that only the active protein catalyzes the isotopic exchange, and forms that contain partially assembled active sites (80−90%) do not give rise to broadening of ^{13}CO due to binding or collisions with CODH-II. Moreover, a Ni-depleted recombinant enzyme and an active site variant that cannot complete the CO oxidation reaction (K563L) are devoid of activity and correspondingly do not exhibit significant ^{13}CO broadening. On the other hand, the C56A variant, which lacks a Cys residue that acts as a ligand to the B-cluster, exhibits ^{13}CO line broadening; however, it is unable to support steady-state CO oxidation because it can only oxidize CO to CO_2, and not transfer electrons to an external electron acceptor. These results strongly indicate that the enzyme-catalyzed process responsible for ^{13}CO line broadening includes the steps of CO binding and oxidation to bound CO_2, reduction of bound CO_2 back to CO, and dissociation of CO; however, the process does not include release of bound CO_2 or electron transfer through the internal electron transfer chain involving the B- and C-clusters. Thus, CO_2 remains bound at the active site before it is more slowly released into solution. A bridging mode of CO_2 binding between the Ni and Fe has been recently proposed (*38*), and evidence for a CO_2 binding site(s) has been offered by FTIR studies (*44*). Since oxidization of CO by CODH follows a ping-pong kinetic mechanism (*17*), CO_2 release must occur prior to binding of external electron acceptors.

Our results also provide insight into the mechanism of release of the two protons generated as a product of CO oxidation, as shown in eq 1. Like CO-dependent methyl viologen reduction, where k_{H_2O}/k_{D_2O} equals 0.85, the exchange between free ^{13}CO and CODH-bound $^{13}CO_2$ exhibits a small solvent isotope effect of 0.87 and does not exhibit a strong buffer effect within the range of 0.1−1 M buffer (Table 1). In addition, although CO oxidation is strongly pH-dependent, there is no effect of pD on ^{13}CO exchange broadening. The absence of a pD effect and the minimal solvent kinetic isotope and buffer effects suggest that steps involving transfer of a proton to solution do not occur during the ^{13}CO exchange. These results are significant because they provide evidence that during the reactions that lead to the exchange broadening, as shown in eq 8, the protons produced during the oxidation of CO to CO_2 remain at the active site and are recycled in the subsequent reduction of bound CO_2 to regenerate CO. Furthermore, the results indicate that the release of protons to solvent occurs after the oxidation of CO at the C-cluster during the steady-state CO oxidation reaction. This situation is similar to that of carbonic anhydrase, where similar isotope exchange experiments identified reservoirs for protons at the active site that were later confirmed by various structure−function studies (*45–48*). For CODH, it is likely that the proton transfer network that has been proposed for CODH (*8, 36*), which includes lysine and histidine residues in provocative positions at the active site, accounts for this proton reservoir.

The exchange broadening phenomenon is comprised of all forward and reverse steps shown in eq 8. The magnitude of the broadening need not be higher than the k_{cat} for CO oxidation because steps involving conversion of $CODH_{red}-{}^{13}CO_2$ to $CODH_{ox}-{}^{13}CO$ and subsequent release of ^{13}CO must occur during exchange broadening of ^{13}CO but not during CO oxidation. However, all the steps occurring during exchange broadening must also occur during the isotopic exchange process. Since the isotope exchange is much slower (2 s^{-1}) than exchange broadening (1100 s^{-1}), either release of CO_2 from $CODH_{red}-CO_2$ or re-uptake of CO_2 from solvent slows the exchange by that amount, i.e., 550-fold. Moreover, since CO_2 release must occur at a rate higher than 1500 s^{-1} (k_{cat} for CO oxidation), it is likely that the re-uptake of CO_2 is the step with a rate constant of 2 s^{-1} that is rate-limiting for both the isotope exchange between CO and CO_2 in solution and reduction of CO_2 to CO.[6]

The intramolecular electron transfer steps within CODH-II are expected to occur at rates of $\sim 10^5$ s^{-1} (*49, 50*), since the edge-to-edge distances between the D- and B-clusters and between the B- and C-clusters are 11 and 10 Å, respectively (*14*). Thus, intermolecular electron transfer to external mediators is the likely step that limits k_{cat} for oxidation of CO by CODH-II. Indeed, the specific activity of CODH-II was found to be dependent on the nature of the electron acceptor used in the assays (*2*). While k_{cat} is strongly pH-dependent, this parameter does not exhibit a substantial kinetic solvent isotope effect (Supplementary Figure 3); thus, a proton release step is not concurrent with re-oxidation of the enzyme by external electron acceptors.

The first step in the CO oxidation mechanism involves diffusion and/or migration of CO to the C-cluster at the active site. To obtain information about this diffusional process, we used CN^- as a CO surrogate because it binds like CO to the C-cluster but does not undergo redox chemistry; instead, it simply releases and equilibrates with CN^- in solution. The $^{13}CN^-$ isotope exchange reaction is 30-fold faster than the rate of the ^{13}CO exchange broadening (1100 s^{-1}). Assuming that CO and CN^- use the same channel, this provides a limiting rate for movement of CO through the channel. We suggest that the $^{13}C-{}^{12}CN^-$ exchange reaction in conjunction with site-directed mutagenesis could be used to identify residues that line the CO channel.

The $^{13}CN^-$ exchange broadening occurs much faster than that for ^{13}CO, most likely because the $^{13}CN^-$ exchange needs to involve only the migration of CN^- to the active site and binding of CN^- to the enzyme and release of CN^- from the enzyme. A surprising result is that the rate of $^{13}CN^-$ exchange decreased much less in the Ni-depleted enzyme than the rate of ^{13}CO exchange. One possibility is that CN^- binds to the Fe1 subsite of the C-cluster, as proposed earlier (*41*), while CO binds to Ni. However, there is substantial kinetic and

[6] Both isotopic and broadening exchange processes are occurring simultaneously in the experiments described herein.

XAS evidence that CN^- binds to Ni (*38, 39*). Another possibility is that there are two binding sites for CN^-. Various studies indicate that cyanide is a slow binding inhibitor of CODH (*39, 42*). Furthermore, Morton modeled slow binding CN^- inhibition as a two-step process involving a rapid reversible reaction followed by a slow step in which CN^- is very slowly released from the enzyme (*42*). In this model, the second step is responsible for the tight binding. Perhaps the first step involves binding of CN^- to one or more sites in the CO channel in a rapid exchanging regime that we could observe by NMR. The second step, perhaps involving coordination of CN^- to Ni, would not contribute to the NMR-monitored exchange because its off rate is too slow (<0.01 s^{-1}). Thus, removal of Ni could affect the structure of the channel and, thus, slow the rapid cyanide exchange ~10-fold, but not as much as it would affect the slow exchange (invisible to the NMR-monitored exchange). This situation is similar to the rapid ^{13}CO exchange broadening in which we observe by NMR the steps preceding the slow release and re-uptake of CO_2 release. Thus, perhaps in the case of the CN^- exchange, the NMR experiments monitor the steps preceding ligation of CN^- to Ni, i.e., migration of CN^- between solution and the CO channel. Thus, the $^{13}CN^-$ exchange may be a rather direct measure of the rate of movement of CO through the channel in CODH.

ACKNOWLEDGMENT

We are enormously indebted to Sara Basiaga and Matthew Shortridge of the NMR Facility at the Chemistry Department of the University of Nebraska for the time and effort spent recording the spectra reported herein. We thank Brady Brabec, Elizabeth Pierce, and Dr. Matthias Anthoine for the generation and purification of the CODH-II_{HT} mutants. We are also grateful to Drs. Gil Navon and Joseph Dumais for helpful discussions on NMR and Dr. Ashraf Raza for the mass spectrometry analysis of recombinant CODH-II_{HT}.

SUPPORTING INFORMATION AVAILABLE

Three figures showing the dependence of CODH activity on CO_2 concentration, the solvent isotope effect on the CO oxidation reaction, and the bicarbonate dependence of the CO oxidation reaction. This material is available free of charge via the Internet at http://pubs.acs.org.

REFERENCES

1. Bloembergen, N., Purcell, E. M., and Pound, R. V. (1948) Relaxation Effects in Nuclear Magnetic Resonance Absorption. *Phys. Rev. 73*, 679–712.
2. Svetlitchnyi, V. P. C. A. G., and Meyer, O. (2001) Two Membrane-Associated NiFeS-Carbon Monoxide Dehydrogenases from the Anaerobic Carbon-Monoxide-Utilizing Eubacterium Carboxydothermus hydrogenoformans. *J. Bacteriol. 183*, 5134–5144.
3. Drake, H. L. (1994) *Acetogenesis*, Chapman & Hall, New York.
4. Wu, M., Ren, Q., Durkin, A., Daugherty, S., Brinkac, L., Dodson, R., Madupu, R., Sullivan, S., Kolonay, J., Haft, D., Nelson, W., Tallon, L., Jones, K., Ulrich, L., Gonzalez, J., Zhulin, I., Robb, F., and Eisen, J. (2005) Life in hot carbon monoxide: The complete genome sequence of *Carboxydothermus hydrogenoformans* Z-2901. *PLoS Genet. 1*, e65.
5. Gnida, M., Ferner, R., Gremer, L., Meyer, O., and Meyer-Klaucke, W. (2003) A novel binuclear [CuSMo] cluster at the active site of carbon monoxide dehydrogenase: Characterization by X-ray absorption spectroscopy. *Biochemistry 42*, 222–230.
6. Ragsdale, S. W. (2004) Life with Carbon Monoxide. *Crit. Rev. Biochem. Mol. Biol. 39*, 165–195.
7. Singer, S. W., Hirst, M. B., and Ludden, P. W. (2006) CO-dependent H_2 evolution by *Rhodospirillum rubrum*: Role of CODH: CooF complex. *Biochim. Biophys. Acta 1757*, 1582–1591.
8. Drennan, C. L., Heo, J., Sintchak, M. D., Schreiter, E., and Ludden, P. W. (2001) Life on carbon monoxide: X-ray structure of *Rhodospirillum rubrum* Ni-Fe-S carbon monoxide dehydrogenase. *Proc. Natl. Acad. Sci. U.S.A. 98*, 11973–11978.
9. Jeoung, J. H., and Dobbek, H. (2007) Carbon dioxide activation at the Ni,Fe-cluster of anaerobic carbon monoxide dehydrogenase. *Science 318*, 1461–1464.
10. Ragsdale, S. W. (1997) The Eastern and Western branches of the Wood/Ljungdahl pathway: How the East and West were won. *BioFactors 9*, 1–9.
11. Lindahl, P. A. (2002) The Ni-containing Carbon Monoxide Dehydrogenase Family: Light at the End of the Tunnel. *Biochemistry 41*, 2097–2105.
12. Darnault, C., Volbeda, A., Kim, E. J., Legrand, P., Vernede, X., Lindahl, P. A., and Fontecilla-Camps, J. C. (2003) Ni-Zn-[Fe4-S4] and Ni-Ni-[Fe4-S4] clusters in closed and open subunits of acetyl-CoA synthase/carbon monoxide dehydrogenase. *Nat. Struct. Biol. 10*, 271–279.
13. Doukov, T. I., Iverson, T. M., Seravalli, J., Ragsdale, S. W., and Drennan, C. L. (2002) A Ni-Fe-Cu center in a bifunctional carbon monoxide dehydrogenase/acetyl-CoA synthase. *Science 298*, 567–572.
14. Dobbek, H. S. V., Gremer, L., Huber, R., and Meyer, O. (2001) Crystal structure of a carbon monoxide dehydrogenase reveals a [Ni-4Fe-5S] cluster. *Science 203*, 1281–1285.
15. Rees, D. C., and Howard, J. B. (2000) Nitrogenase standing at the crossroads. *Curr. Opin. Chem. Biol. 4*, 559–566.
16. Howard, J. B., and Rees, D. C. (2006) How many metals does it take to fix N2? A mechanistic overview of biological nitrogen fixation. *Proc. Natl. Acad. Sci. U.S.A. 103*, 17088–17093.
17. Seravalli, J., Kumar, M., Lu, W. P., and Ragsdale, S. W. (1995) Mechanism of CO oxidation by carbon monoxide dehydrogenase from *Clostridium thermoaceticum* and its inhibition by anions. *Biochemistry 34*, 7879–7888.
18. Anderson, M. E., and Lindahl, P. A. (1996) Spectroscopic states of the CO oxidation/CO_2 reduction active site of carbon monoxide dehydrogenase and mechanistic implications. *Biochemistry 35*, 8371–8380.
19. Seravalli, J., Kumar, M., Lu, W. P., and Ragsdale, S. (1997) The mechanism of carbon monoxide oxidation by the carbon monoxide dehydrogenase/acetyl-CoA synthase from *Clostridium thermoaceticum*: Kinetic characterization of the intermediates. *Biochemistry 36*, 11241–11251.
20. Ragsdale, S. W. (2006) Metals and their scaffolds to promote difficult enzymatic reactions. *Chem. Rev. 106*, 3317–3337.
21. Fraser, D. M. L. P. A. (1999) Evidence for a proposed intermediate redox state in the CO/CO_2 active site of acetyl-CoA synthase (carbon monoxide dehydrogenase) from *Clostridium thermoaceticum*. *Biochemistry 38*, 15706–15711.
22. Parkin, A., Seravalli, J., Vincent, K. A., Ragsdale, S. W., and Armstrong, F. A. (2007) Rapid electrocatalytic CO_2/CO interconversions by *Carboxydothermus hydrogenoformans* CO dehydrogenase I on an electrode. *J. Am. Chem. Soc. 129*, 10328–10329.
23. Koenig, S., and Brown, R. (1973) Kinetic Parameters of Human Carbonic Anhydrase A as determined from the linewidths in CO_2 and HCO_3^-. *Biochem. Biophys. Res. Commun. 53*, 624–630.
24. Koenig, S., and Brown, R. (1974) The Kinetic Parameters of Carbonic Anhydrase by ^{13}C NMR. *Pure Appl. Chem. 40*, 103–113.
25. Simonsson, I., Jonsson, B. H., and Lindskog, S. (1979) A ^{13}C Nuclear-Magnetic-Resonance Study of CO_2-HCO_3 Exchange Catalyzed by Human Carbonic Anhydrase C at Chemical Equilibrium. *Eur. J. Biochem. 93*, 409–417.
26. Simonsson, I., Jonsson, B. H., and Lindskog, S. (1982) A ^{13}C Nuclear Magnetic Resonance Study of CO_2/HCO_3 Exchange Catalyzed by Human Carbonic Anhydrase I. *Eur. J. Biochem. 129*, 165–169.
27. Pocker, Y., and Bjorkquist, D. W. (1977) Comparative Studies of Bovine Carbonic Anhydrase in H_2O and D_2O. Stopped-Flow Studies of the Kinetics of Interconversion of CO_2 and HCO_3^-. *Biochemistry 16*, 5698–5707.
28. Rowlett, R., and Silverman, D. (1982) Kinetics of the Protonation of Buffer and Hydration of CO_2 Catalyzed by Human Carbonic Anhydrase II. *J. Am. Chem. Soc. 104*, 6737–6741.

29. Brandner, J. D., and Urey, H. C. (1945) Kinetics of the Isotopic Exchange Reaction between Carbon Monoxide and Carbon Dioxide. *J. Chem. Phys. 13*, 351–362.
30. Norris, T. H., and Ruben, S. (1950) Kinetics of the Isotope Exchange Reaction between Carbon Monoxide and Carbon Dioxide. *J. Chem. Phys. 18*, 1595–1600.
31. Gu, W. S. J., Ragsdale, S. W., and Cramer, S. P. (2004) CO-induced structural rearrangement of the C-cluster in *Carboxydothermus hydrogenoformans* CO dehydrogenase: Evidence from Ni K-edge X-ray absorption spectroscopy. *Biochemistry 43*, 9029–9035.
32. Elliott, J. I., and Brewer, J. M. (1978) The inactivation of yeast enolase by 2,3-butanedione. *Arch. Biochem. Biophys. 190*, 351–357.
33. Freney, A., and Burgen, A. S. V. (1973) Cyanide Binding to Carbonic Anhydrase: A ^{13}C-Nuclear-Magnetic-Resonancee Study. *Eur. J. Biochem. 34*, 107–111.
34. Juneja, J., Bhavesh, N. S., Udgaonkar, J. B., and Hosur, R. V. (2002) NMR Identification and Characterization of the Flexible Regions in the 160 kDa Molten Globule-Like Aggregate of Barstar at Low pH. *Biochemistry 41*, 9885–9899.
35. Kumar, M., Lu, W.-P., and Ragsdale, S. W. (1994) Binding of carbon disufide to the site of acetyl-CoA synthesis by the nickel-iron-sulfur protein, CO dehydrogenase, from *Clostridium thermoaceticum*. *Biochemistry 33*, 9769–9777.
36. Kim, E. J., Feng, J., Bramlett, M. R., and Lindahl, P. A. (2004) Evidence for a Proton Transfer Network and a Required Persulfide-Bond-Forming Cysteine Residue in Ni-Containing Carbon Monoxide Dehydrogenases. *Biochemistry 43*, 5728–5734.
37. Ensign, S. A., Bonam, D., and Ludden, P. W. (1989) Nickel is required for the transfer of electrons from carbon monoxide to the iron-sulfur center(s) of carbon monoxide dehydrogenase from *Rhodospirillum rubrum*. *Biochemistry 28*, 4968–4973.
38. Ha, S.-H., Korbas, M., Klepsch, M., Meyer-Klaucke, W., Meyer, O., and Svetlitchnyi, V. (2007) Interaction of Potassium Cyanide with the [Ni-4Fe-5S] Active Site Cluster of CO Dehydrogenase from *Carboxydothermus hydrogenoformans*. *J. Biol. Chem. 282*, 10639–10646.
39. Ensign, S. A., Hyman, M. R., and Ludden, P. W. (1989) Nickel-specific, slow binding inhibition of carbon monoxide dehydrogenase from *Rhodospirillum rubrum* by cyanide. *Biochemistry 28*, 4973–4979.
40. Anderson, M. E., and Lindahl, P. A. (1994) Organization of clusters and internal electron pathways in CO dehydrogenase from *Clostridium thermoaceticum*: Relevance to the mechanism of catalysis and cyanide inhibition. *Biochemistry 33*, 8702–8711.
41. DeRose, V. J., Telser, J., Anderson, M. E., Lindahl, P. A., and Hoffman, B. M. (1998) A Multinuclear ENDOR Study of the C-Cluster in CO Dehydrogenase from *Clostridium thermoaceticum*: Evidence for HxO and Histidine Coordination to the [Fe4S4] Center. *J. Am. Chem. Soc. 120*, 8767–8776.
42. Morton, T. A. (1991) Sequencing and active site studies of carbon monoxide dehydrogenase/acetyl-CoA synthase from *Clostridium thermoaceticum*. Ph.D. Thesis, University of Georgia, Athens, GA.
43. Lin, Y., Gerfen, G. J., Rousseau, D. L., and Yeh, S. R. (2003) Ultrafast microfluidic mixer and freeze-quenching device. *Anal. Chem. 75*, 5381–5386.
44. Cheng, J., Huang, S., Seravalli, J., Gutzman, H.-J., Schwartz, D., Ragsdale, S. W., and Bagley, K. (2003) Infrared studies of carbon monoxide binding to carbon monoxide dehydrogenase/acetyl-CoA synthase from *Moorella thermoacetica*. *Biochemistry 42*, 14822–14830.
45. Fisher, S. Z., Maupin, C. M., Budayova-Spano, M., Govindasamy, L., Tu, C., Agbandje-McKenna, M., Silverman, D. N., Voth, G. A., and McKenna, R. (2007) Atomic crystal and molecular dynamics simulation structures of human carbonic anhydrase II: Insights into the proton transfer mechanism. *Biochemistry 46*, 2930–2937.
46. Fisher, S. Z., Hernandez-Prada, J. A., Duda, D., Yoshioka, C., An, H., Govindasamy, L., Silverman, D. N., and McKenna, R. (2005) Structural and kinetic characterization of active-site histidine as a proton shuttle in catalysis by human carbonic anhydrase II. *Biochemistry 44*, 1097–1105.
47. Tu, C. K., Silverman, D., Forsman, C., Jonsson, B. H., and Lindskog, S. (1989) Role of histidine 64 in the catalytic mechanism of human carbonic anhydrase II studied with a site-specific mutant. *Biochemistry 28*, 7913–7918.
48. Duda, D., Tu, C., Qian, M., Laipis, P., Agbandje-McKenna, M., Silverman, D. N., and McKenna, R. (2001) Structural and kinetic analysis of the chemical rescue of the proton transfer function of carbonic anhydrase II. *Biochemistry 40*, 1741–1748.
49. Page, C. C., Keske, J. M., Warncke, K., Farid, R. S., and Dutton, P. L. (1992) Nature of biological electron transfer. *Nature 355*, 796–802.
50. Page, C. C., Moser, C. C., Chen, X., and Dutton, L. (1999) Natural engineering principles of electron tunnelling in biological oxidation-reduction. *Nature 402*, 47–52.

BI8004522